PERGAMON

Chemical Engineering Science 58 (2003) 2893–2902

Chemical Engineering Science

www.elsevier.com/locate/ces

Particle size distributions and viscosity of suspensions undergoing shear-induced coagulation and fragmentation

G. Barthelmes[a], S. E. Pratsinis[a,*], H. Buggisch[b]

[a] *Particle Technology Laboratory, Department of Mechanical and Process Engineering, Sonneggstrasse 3, ML F25, ETH Zürich, CH-8092 Zürich, Switzerland*

[b] *Institut für Mechanische Verfahrenstechnik und Mechanik, Universität Karlsruhe (TH), D-76128 Karlsruhe, Germany*

Received 23 September 2002; received in revised form 13 December 2002; accepted 21 February 2003

Abstract

The dynamic behavior of concentrated suspensions (up to a solids volume fraction of 20%) of non-spherical particles is investigated theoretically by coupling a rheological law to a population balance model accounting for coagulation and fragmentation of the detailed particle size distribution. In these suspensions, the immobilization of matrix liquid renders the viscosity dependent on the particle aggregation state. The effect of initial solids volume concentration and shear rate on the transient behavior of particle size distribution and suspension viscosity is examined. Power law correlations for the equilibrium flow curves of aggregating suspensions are deduced and compared to experimental data. Steady-state or equilibrium particle size distributions are found to be self-preserving with respect to solids volume fraction and shear rate.

Keywords: Particles; Fractals; Self-preserving; Population balance; Modeling; Rheology

1. Introduction

Simultaneous coagulation (or aggregation) and fragmentation by fluid shear is encountered in processes involving polymerization (Blatz & Tobolsky, 1945), liquid–liquid dispersion (Coulaloglou & Tavlarides, 1977), emulsification (Danov, Ivanov, Gurkov, & Borwankar, 1994), flocculation (Ives, 1978) and even diesel soot formation (Harris & Maricq, 2002). At low particle concentrations the fluid and particle dynamics can be decoupled, facilitating thus the description of the suspension dynamics (e.g. Spicer & Pratsinis, 1996a).

At high solids concentrations, however, the state of particle aggregation can affect the rheology as has been encountered in polymer slurry processing (Horn & Patterson, 1997), metallic alloy solidification (Barbé, Perez, & Papoular, 2000), food processing (Weipert, Tscheuschner, & Windhab, 1993) and even blood circulation (Schmid-Schönbein, Gallasch, Gosen, Volger, & Klose, 1976). Aggregates immobilize part of the matrix fluid inside them and therefore increase the effective solids volume fraction in the suspension and its viscosity (Graham, Steele, & Bird, 1984; Tsutsumi, Yoshida, Yui, Kanamori, & Shibata, 1994). Increasing the viscosity increases the shear stresses that enhance breakage of aggregates. The structure of the aggregates and, thus, the rheology strongly depends on the applied shear stresses.

Aggregating suspensions show shear thinning behavior even with Newtonian matrix liquids. At low shear rates their viscosity–shear rate correlation can be approximated by power laws (Doi & Chen, 1989; Chen & Doi, 1989). A variation of the primary particle concentration (Chen & Doi, 1989; Folkersma, van Diemen, Laven, & Stein (1999)) or interparticle forces (Kurzbeck, Kaschta, & Münstedt, 1996) leads to a parallel shift of the flow curves in the low shear rate region. At higher shear rates, the flow curves level off to a Newtonian plateau, which is the state of a deaggregated suspension where the aggregates can no longer break (Snabre & Mills, 1996). Rheological studies on aggregating suspensions mainly consider equilibrium, when the aggregate structure is fully developed and in steady state. de Rooij, Potanin, van den Ende, and Mellema (1994), in particular, studied the transient rheological behavior of aggregating

* Corresponding author. Tel.: +41-1-632-2510; fax: +41-1-632-1595.
E-mail address: pratsinis@ptl.mavt.ethz.ch (S. E. Pratsinis).

0009-2509/03/$ - see front matter © 2003 Elsevier Science Ltd. All rights reserved.
doi:10.1016/S0009-2509(03)00133-7

suspensions of polystyrene latex. They pre-sheared the suspensions at high shear rate for complete deaggregation and then reduced sharply the shear rate resulting in a pronounced viscosity increase and later on in a shear rate-dependent equilibrium viscosity.

Here, the dynamic behavior of suspensions of polydisperse particles is examined accounting for shear-driven coagulation and fragmentation by population balances. Fluid and particle dynamics are coupled by replacing the solids concentration in material laws with an effective solids volume fraction which includes the immobilized fluid (Wolthers, van den Ende, Duits, & Mellema, 1996). That way it overcomes the limitations of the earlier models of de Rooij et al. (1993, 1994) that were confined to monodisperse particle suspensions and of Kramer and Clark (1999) that assumed constant viscosity. The suspension dynamics are investigated at various initial solids fractions and shear rates and the transient behavior of representative macroscopic quantities (mass mean diameter, effective concentration, viscosity) is studied. Special focus is placed on the equilibrium state, particularly on a sensitivity analysis of various model parameters on the flow curves, which are compared to experimental data.

2. Theory

2.1. Sectional population balance model

The evolution of aggregate size distributions undergoing simultaneous coagulation and fragmentation is described by the population balance equation (Blatz & Tobolsky, 1945). To solve this equation, Spicer and Pratsinis (1996a) extended the sectional model of Hounslow, Ryall, and Marshall (1988) to account for fragmentation of aggregates. They used a sectional spacing factor $V_i/V_{i-1} = 2$, where V_i is the mass-equivalent volume of an aggregate in section i, i.e. the volume of a fully coalesced aggregate that consists of $x_i = 2^{i-1}$ spherical monodisperse primary particles of diameter d_p:

$$V_i = \frac{\pi}{6} d_i^3 = x_i\, v_p = x_i\, \frac{\pi}{6}\, d_p^3. \tag{1}$$

With this sectionalization, the population balance for the number concentration N_i of aggregates in section i becomes (cf. Spicer & Pratsinis, 1996a):

$$\begin{aligned}\frac{\mathrm{d}N_i}{\mathrm{d}t} = &\sum_{j=1}^{i-2} 2^{j-i+1} \beta_{i-1,j}\, N_{i-1} N_j + \frac{1}{2}\, \beta_{i-1,i-1}\, N_{i-1}^2 \\ &- N_i \sum_{j=1}^{i-1} 2^{j-i} \beta_{i,j}\, N_j - N_i \sum_{j=i}^{i_{\max}-1} \beta_{i,j}\, N_j \\ &- S_i\, N_i + \sum_{j=i}^{i_{\max}} \Gamma_{i,j}\, S_j\, N_j. \end{aligned} \tag{2}$$

The first two terms of the right-hand side (RHS) describe the "birth" of aggregate particles of section i by coagulation of smaller aggregates, the next two RHS terms account for the "death" of aggregates of section i by coagulation with other aggregates, while the last two RHS terms describe death and birth, respectively, of aggregates in this section by breakage.

The $\beta_{i,j}$ is the so-called collision kernel of particles or aggregates. The collisions can be caused by the ever-present thermal motion (Brownian motion) or by shear deformation of the fluid (Smoluchowski, 1917). Here, only particles of at least micron size are considered where the influence of thermal motion is negligible compared to shear. This collision rate $\beta_{i,j}$ of Saffman and Turner (1956) for homogeneous, isotropic turbulence with spherical particles smaller than the Kolmogorov microscale (for which particle inertia can be neglected) was extended by Flesch, Spicer, and Pratsinis (1999) to account for the aggregate structure:

$$\beta_{i,j} = 0.31\, G\, v_p (x_i^{1/D_f} + x_j^{1/D_f})^3, \tag{3}$$

where G is the so-called shear rate, i.e. the spatially averaged velocity gradient that is constant and homogeneous. The symbol G is utilized for both, laminar and turbulent shear. Possible effects of viscous retardation, van der Waals attraction or particle repulsion are neglected, although attractive and repulsive forces are usually not fully compensating and the collision efficiency is depending on shear rate (cf. Vanni & Baldi, 2002). Here, completely destabilized suspensions are assumed where all collisions are successful. This assumption of a collision efficiency of unity appears realistic as the streamlines of flow only penetrate the outmost layers of compact aggregates (Veerapaneni & Wiesner, 1996). Therefore the primary particle density in the outer regions of the aggregates must be sufficiently large to obtain collisions of primary particles when the aggregates start to overlap. The slight penetration of flow into the aggregate reduces, however, hydrodynamic repulsion found in squeezing flow between two approaching solid spheres (see e.g. Happel & Brenner, 1973 or Kim & Karrila, 1991), which would have decreased the collision efficiency.

Aggregates are irregularly shaped with a void fraction or inversely an aggregate density that depends on aggregate size. As they exhibit fractal-like properties they can be characterized by a fractal dimension D_f (Mandelbrot, 1983). In sheared suspensions the fractal dimension is typically in the range of 2.1–2.7. Here, the fractal dimension is a constant though it can depend on shear rate, shear history (Spicer et al., 1998) and on aggregate size (Oles, 1992). The collision diameter $d_{c,i}$ of an aggregate of section i is related to the number of primary particles x_i of diameter d_p in it, by (cf. Matsoukas & Friedlander, 1991)

$$d_{c,i} = d_p\, x_i^{1/D_f}. \tag{4}$$

The smaller the D_f, the less compact the aggregate is and the larger is its collision diameter.

The fragmentation kernel S_i is the rate of particle breakage and is related to shear rate and aggregate size by (Pandya & Spielman, 1983)

$$S_i = A' G^q V_i^{1/3}, \tag{5}$$

where S_i is proportional to the mass-equivalent diameter $d_i \propto V_i^{1/3} = (x_i v_p)^{1/3}$. The fragmentation parameter A' and the exponent q are determined experimentally (Spicer & Pratsinis, 1996a). Since the aggregates are actually ruptured by the forces acting upon them, the shear rate is replaced by the external shear stress in the suspension. This is similar to the approach of Kramer and Clark (1999) who utilized the product of viscosity and strain rate which is proportional to the shear stress in simple shear flows. The shear stress is proportional to viscosity that depends on the effective volume fraction of the aggregates. A characteristic shear stress τ^* is introduced to non-dimensionalize the shear stress term. It is a measure of the aggregate strength: the larger the τ^*, the less susceptible to breakage are the particles at a certain shear stress:

$$S_i \propto \left(\frac{\eta G}{\tau^*}\right)^q. \tag{6}$$

A comparison of Eqs. (5) and (6) shows that τ^* can be related to A' by

$$\tau^* = \left(\frac{k_b}{A'}\right)^{1/q} \eta, \tag{7}$$

where $k_b = 1\ \mathrm{cm}^{-1}\ \mathrm{s}^{-1}$ is used to match the dimensions of both sides of the equation. From the data of Oles (1992) for an aqueous dilute polystyrene suspension, Spicer and Pratsinis (1996a) extracted $A' = 0.0047\ \mathrm{cm}^{-1}\ \mathrm{s}^{q-1}$ and $q = 1.6$. With the viscosity of water $\eta = 10^{-3}$ Pa s, this results in a characteristic shear stress $\tau^* = 0.0285$ Pa.

As the disrupting shear forces are acting on the collision diameter of the aggregate, the mass equivalent diameter d_i is replaced by the collision diameter $d_{c,i}$ in Eq. (5). However, aggregates with identical collision diameter but lower fractal dimension are more porous. Thus they contain less particle bonds per aggregate volume and their strength is lower (Tang, Ma, & Shiu, 2001). So they are ruptured more easily by shear forces. Therefore, the linear dependency on the aggregate collision diameter can be replaced by a power law so the breakage rate increases with decreasing fractal dimension, i.e. with increasing porosity of the aggregates.

$$S_i \propto v_p^{1/3} \left(\frac{\mathrm{d}_{c,i}}{\mathrm{d}_p}\right)^{3/D_f}. \tag{8}$$

This is consistent with Pandya and Spielman (1982) who proposed $S \propto V^m$ where the exponent m is determined experimentally (for their data: $m = 0.33$). As porosity is independent of the primary particle size, the volume of the primary particles is distinguished from the relative aggregate size. Introducing Eqs. (6)–(8) in Eq. (5), it becomes

$$S_i = k_b \left(\frac{\eta(\phi_{\mathrm{tot}})\, G}{\tau^*}\right)^q v_p^{1/3} \left(\frac{\mathrm{d}_{c,i}}{\mathrm{d}_p}\right)^{3/D_f}. \tag{9}$$

In dilute suspensions ($\phi \to 0$), where the viscosity is constant, and for spherical particles ($D_f = 3$), Eq. (9) nicely reduces to Eq. (5).

The viscosity of suspensions with fractal-like aggregates corresponds to that of suspensions of solid spheres with the hydrodynamic diameter of the aggregates (Snabre & Mills, 1996). There is a variety of correlations between particle volume fraction and suspension viscosity (Quemada, 1977). Here, a one-parameter viscosity function is chosen that describes polydisperse suspensions of hard spheres (Quemada, 1977) or of "structural units" like clusters or aggregates (Quemada, 1998):

$$\eta(\phi_{\mathrm{tot}}) = \frac{\eta_0}{(1 - \phi_{\mathrm{tot}}/\phi_m)^2}. \tag{10}$$

In this equation, ϕ_{tot} is the effective or total volume concentration of the aggregates:

$$\phi_{\mathrm{tot}} = \sum_{i=1}^{i_{\max}} N_i\, v_{c,i}, \tag{11}$$

where $v_{c,i} = (\pi/6)\, d_{c,i}^3$ is the collision volume of the aggregates. The ϕ_m is the maximum volume concentration at which the viscosity diverges to infinity, ranging from 0.58 (Wolthers et al., 1996) to 0.69 (Lee, So, & Yang, 1999), while $\phi_m = 0.6$ is used here as an average.

The fragment distribution function $\Gamma_{i,j}$ in Eq. (2) gives the fraction of fragments produced in section i, when an aggregate of section j breaks. Here only binary breakage (or "aggregate splitting") is considered, with

$$\Gamma_{i,j} = \begin{cases} 2, & j = i + 1, \\ 0 & \text{else.} \end{cases} \tag{12}$$

This splitting into two roughly equally sized fragments is consistent with photographic observations by van de Ven (1989) and simulations by Higashitani and Iimura (1998). Splitting into more than two daughter fragments can be considered easily as in Spicer and Pratsinis (1996a).

The width of the aggregate size distribution can be described by a number-based geometric standard deviation σ_{gn} or by a volume based geometric standard deviation σ_{gv}. The σ_{gn} is given by (Hinds, 1999)

$$\ln \sigma_{gn} = \left(\frac{\sum n_i (\ln d_i - \ln d_{gn})^2}{\sum n_i}\right)^{1/2}, \tag{13}$$

where the geometric mean diameter is defined by

$$\ln d_{gn} = \frac{\sum n_i \ln d_i}{\sum n_i}. \tag{14}$$

The volume-based geometric standard deviation σ_{gv} is obtained likewise by replacing n_i by $n_i V_i$ in Eqs. (13) and (14).

The sectional population balance equation (2) for $i_{max}=40$ and the above-defined kernels (3) and (9) and the correlations (10)–(12) is solved numerically using the *VODPK* solver (Byrne, 1992; Netlib, 2001).

3. Results and discussion

3.1. Dynamics of aggregate size distributions

Table 1 shows the parameters employed here. The model was evaluated first for dilute suspensions ($\phi \to 0$) of spherical particles with $D_f = 3$ at the conditions of Oles (1992). The evolution of the detailed size distribution and the mass mean particle diameter as well as the attainment of equilibrium size distribution were identical to that of Spicer and Pratsinis (1996a).

Initially aggregate-free suspensions of particles of $d_p = 2$ μm and $\phi_0 = 0.01$ are considered. Fig. 1 shows the evolution of the dimensionless aggregate mass distribution over d_i. Starting with the initial monodisperse primary particles, first small aggregates of $D_f = 2.3$ are formed ($t^* = t\,G\,\phi_0 = 0.5$) with a low collision cross-section and thus a slow growth. Particle growth accelerates when larger fractal-like aggregates are formed since the newly formed aggregates have a larger collision volume than the sum of the collision volumes of their predecessors, resulting in the large-aggregate mode in the size distribution. This mode can be observed after some time ($t^* = 0.7$) as a hump in the distribution. This hump grows rapidly and moves to smaller sizes ($t^* = 0.8$) because the large aggregates have a high porosity and thus a low strength (Tang et al., 2001).

Table 1
Parameters used for simulation of figures (unless otherwise noted)

Parameter	Figs. 1–6 and 9	Figs. 7 and 8
External		
d_p	2.0 μm	5.1 μm
η_0	10^{-3} Pa s	24×10^{-3} Pa s
ϕ_0	0.01 (Figs. 1–3); 0.1 (Figs. 4, 9)	0.17
G	10 s^{-1} (Figs. 1, 2, 4, 5); 1 s^{-1} (Fig. 3)	—
Model		
D_f	2.3	2.3
q	4	4
τ^*	0.1 Pa (Figs. 1, 2, 4–6); 0.01 Pa (Figs. 3, 9)	16 Pa (Fig. 8)

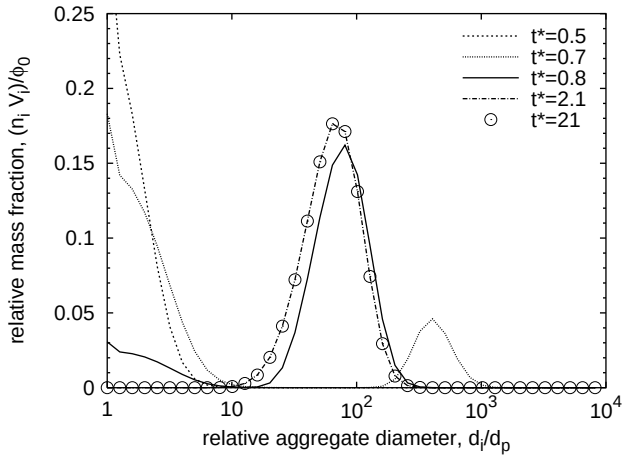

Fig. 1. Particle size distribution at increasing dimensionless time $t^* = t\,G\,\phi_0$ and $D_f = 2.3$ in a moderately concentrated suspension (primary particle concentration $\phi_0 = 0.01$), starting with a completely deaggregated suspension.

Therefore, they are disrupted by the increasing shear forces from the increasing viscosity. After about $t^* = 2.1$, differences in distribution curves can no longer be discerned (cf. $t^* = 2.1$ and 21), i.e. the suspension has reached steady state or equilibrium between particle coagulation and fragmentation.

Transiently (e.g. around $t^* = 0.7$), the distribution curves undergo significant changes in shape by the presence of a significant fraction of primary particles and the appearance of the large aggregate mode. The observation of the very large aggregates or superclusters is in agreement with simulations of Silbert, Melrose, and Ball (1999), who calculated a transient particle gel network that is subsequently ruptured by the ongoing shear forces. Gustafsson, Nordenswan, and Rosenholm (2001) explained also their experimental results on the shear history dependence of aggregating suspensions using the concept of transient gelation.

The shape of the steady-state or equilibrium particle size distributions is independent of the initial solids volume fraction or shear rate (Fig. 2). When these are plotted as a function of a normalized aggregate size, i.e. of the mass-equivalent aggregate diameter d_i of the aggregates divided by the mass mean diameter d_{mm}, all distribution curves collapse to one line. This indicates that steady-state aggregate size distributions are self-preserving with respect to both, initial solids volume fraction ϕ_0 and shear rate G. The latter is consistent with results of Spicer and Pratsinis (1996a) for dilute suspensions. Self-preservation here means that particles attain a size distribution of which the shape is invariant with respect to ϕ_0 and G even though the actual size changes. This holds however only as long as the fraction of primary particles is negligible. At high shear rates, when fragmentation dominates resulting in the decomposition of aggregates into primary particles, the self-preservation is no longer valid as has been shown

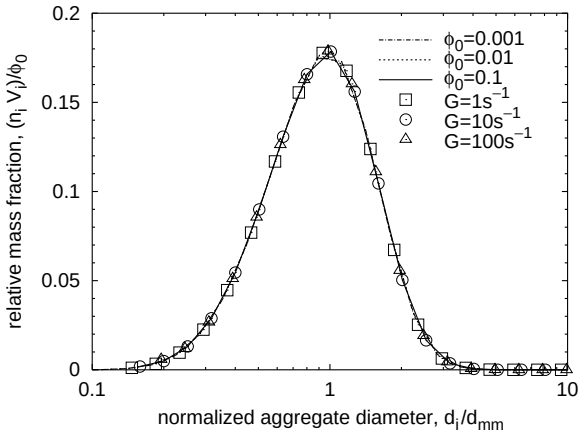

Fig. 2. Normalized particle size distribution for various initial solids volume fractions at $G=10\ s^{-1}$ (lines) and various shear rates at $\phi_0=0.1$ (symbols): ratio of particle mass in one section to total particle mass, as function of the mass-equivalent diameter of the aggregates divided by the mass mean diameter for $D_f=2.3$.

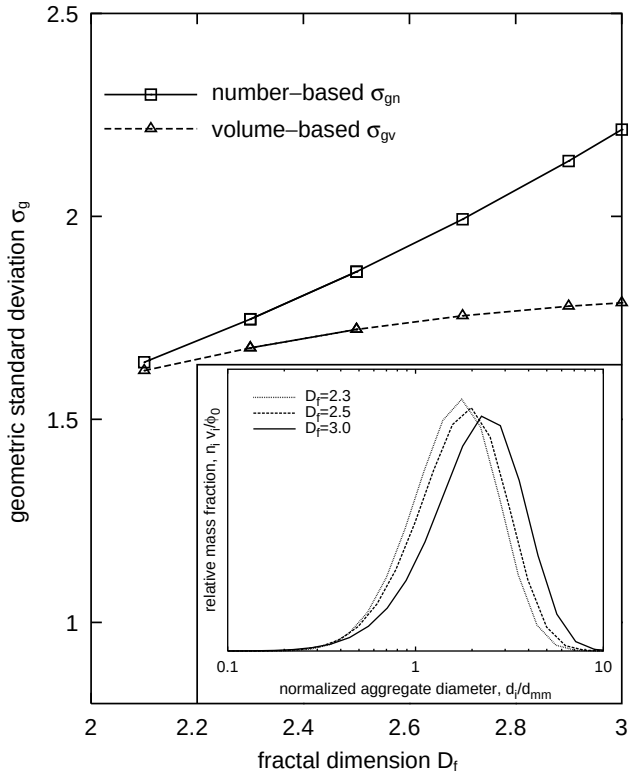

Fig. 3. Geometric standard deviations (number based: σ_{gn}, squares; volume based: σ_{gv}, triangles) of the steady-state particle size distributions as a function of fractal dimension D_f. The inset shows the normalized steady-state particle size distribution by coagulation and fragmentation of concentrated suspensions of $\phi_0=0.01$–0.2 (here: $\phi_0=0.01$) for $D_f=2.3$, 2.5 and 3.

by Spicer, Pratsinis, Trennepohl, and Meesters (1996) for dilute suspensions undergoing shear-induced flocculation.

The inset of Fig. 3 shows the equilibrium or steady-state particle size distributions normalized by d_{mm} for $D_f=2.3$–3, with $\phi_0=0.01$ and $G=1\ s^{-1}$. These normalized steady-state distributions broaden with increasing D_f, so they are not self-preserving with respect to D_f. This behavior of suspensions with shear-induced aggregation and fragmentation is similar to that of suspensions undergoing Brownian coagulation in the continuum regime (Vemury & Pratsinis, 1995). The peak of the distribution curve is sharpened and shifted to smaller sizes for decreasing D_f. The increased fragility of large aggregates at low D_f may dominate over the enhanced collision cross-section narrowing the distributions. In Fig. 3 the number-based geometric standard deviation σ_{gn} (squares) and the volume-based geometric standard deviation σ_{gv} (triangles) are plotted as a function of the fractal dimension. The σ_{gn} decreases from 2.2 for $D_f=3$ to 1.64 for $D_f=2.1$, whereas the dependence of σ_{gv} on D_f is less pronounced (only a decrease from 1.8 to 1.62 for the same D_f). At $D_f=3$, the size distribution and both geometric standard deviations closely coincide with the values of Spicer and Pratsinis (1996a) for binary fragmentation as it is used here. The decrease in σ_{gn} with lower D_f reflects the narrowing of the distributions in the inset of Fig. 3.

Fig. 4 shows the d_{mm} evolution as a function of dimensionless time $t^*=t\,G\,\phi_0$ for various initial volume fractions ϕ_0 (a) and various shear rates (b). With this scaled time, the initial aggregation kinetics coincide regardless of ϕ_0 (Fig. 4a) or G (Fig. 4b). The scaling of the dynamics of shear-induced flocculation of suspensions with $t^*=t\,G\,\phi_0$ has been found in dilute systems also (Oles, 1992; Serra, Colomer, & Casamitjana, 1997). The transient formation of large particles (Fig. 1) results in a short overshoot of the d_{mm} (Fig. 4a and b) at high initial volume fractions (e.g. $\phi_0\geqslant 0.01$) and low shear rates (e.g. $G\leqslant 10\ s^{-1}$). Later on the d_{mm} reaches asymptotically an equilibrium diameter depending on the initial primary particle concentration and on the shear rate as has been shown amply with dilute suspensions (Oles, 1992; Serra et al., 1997). The fractal aggregates tend to occupy as much space as possible, i.e. to establish a space-filling particle network (Folkersma, van Diemen, Laven, van der Plas, & Stein, 1998; Folkersma et al., 1999; Dickinson, 2000). This can be achieved, however, only when the suspension is at rest. Under such conditions, the cluster size scales with (Varadan & Solomon, 2001):

$$\frac{d_{c,i}}{d_p}\propto\phi_0^{1/(D_f-3)}. \tag{15}$$

In sheared concentrated suspensions, the viscosity increases at higher ϕ_{tot} enhancing fragmentation. Therefore, the aggregates become even smaller than at rest and the dependence on ϕ_0 is more pronounced. This result contrasts that of dilute suspensions where increasing particle concentrations give larger steady-state size distributions (Spicer & Pratsinis, 1996b). At high shear rates (e.g. $G=1000\ s^{-1}$), no overshoot in average aggregate size can be observed as the high shear stresses cause high fragmentation rates even of small aggregates.

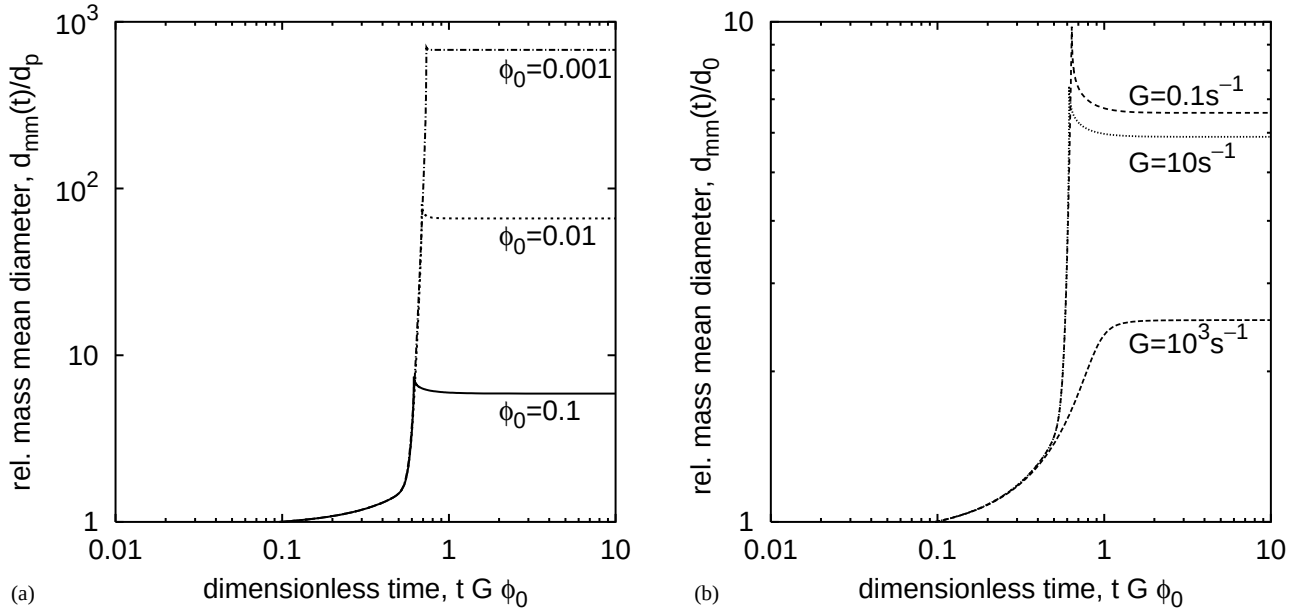

Fig. 4. Evolution of the mass mean diameter as a function of time for various (a) initial solids volume fractions (for $G = 10\ s^{-1}$) and (b) shear rates (for $\phi_0 = 0.1$).

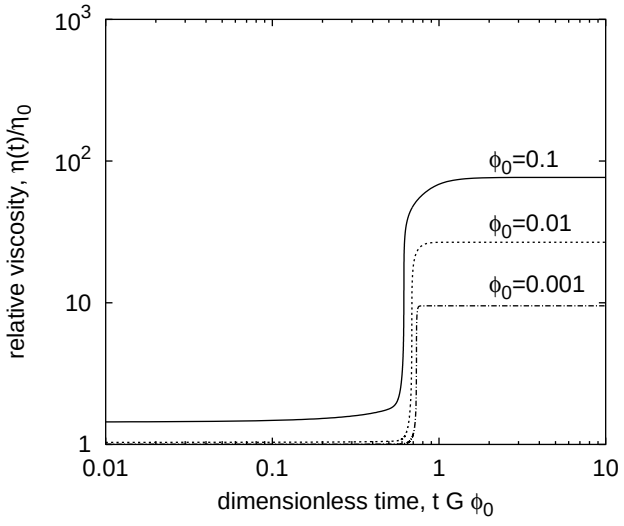

Fig. 5. Evolution of the relative viscosity for the same parameters as in Fig. 4a.

3.2. Viscosity and flow curves

The appearance of the large aggregates leads to an increase in viscosity (Fig. 5). This quantity does not exhibit the overshoot behavior of the mass mean diameter, as only a few of the large particles are formed, but bends smoothly towards an equilibrium value. By coagulation, the fractal aggregates are filling the available space gradually until the simultaneously increasing viscosity is leading to shear stresses that counteract growth by fragmentation. Experimental observations of de Rooij et al. (1994) on the viscosity evolution of aggregating suspensions show moderate slopes of viscosity evolution after a step from high to low shear rate. The very rapid dynamics of viscosity evolution predicted by the model can be attributed to the model assumptions: ideally homogeneous shear field, constant fractal dimension, and completely efficient aggregate collisions.

The correlation between viscosity and applied shear is examined and the influence of various model parameters on the viscosity is elucidated. A common presentation of the rheological properties is the so-called "flow curve" where the suspension viscosity (or the relative viscosity) is plotted against the applied shear rate. To study the influence of the initial volume fraction on the flow curves, ϕ_0 was varied over some range typical for moderately concentrated suspensions (Fig. 6). The simulated flow curves are straight lines in the log–log plot in the range of low shear rates (here $G^* = \eta_0 G/\tau^* \leqslant 1$) and can be approximated by power laws. At high G the viscosity approaches the value of completely deaggregated suspensions. A change of the primary particle concentration causes a parallel shift of the flow curves at low shear rates. This parallel shift of the flow curves is consistent with direct numerical simulations of aggregating concentrated suspensions (Chen & Doi, 1989; Doi & Chen, 1989) and with experimental data of Folkersma et al. (1999) for aqueous polystyrene latex suspensions ($d_p = 2.0\ \mu m$) with 0.5 M NaCl [cf. inset in Fig. 6], and of Zaman, Moudgil, Fricke, and El-Shall (1996) for aqueous silica suspensions ($d_p = 1\ \mu m$) with 0.03 M $NaNO_3$. However, the extend of the parallel shift is underpredicted by the model: The experimental data show an increase of viscosity by more than one order of magnitude when the solids concentration increases from 2% to 10% (de Rooij, Potanin, van den Ende, & Mellema, 1993) or from 3% to 21% (Folkersma et al., 1999), while the model predicts only an increase by a factor of 3 when the solids concentration is increased from 1% to

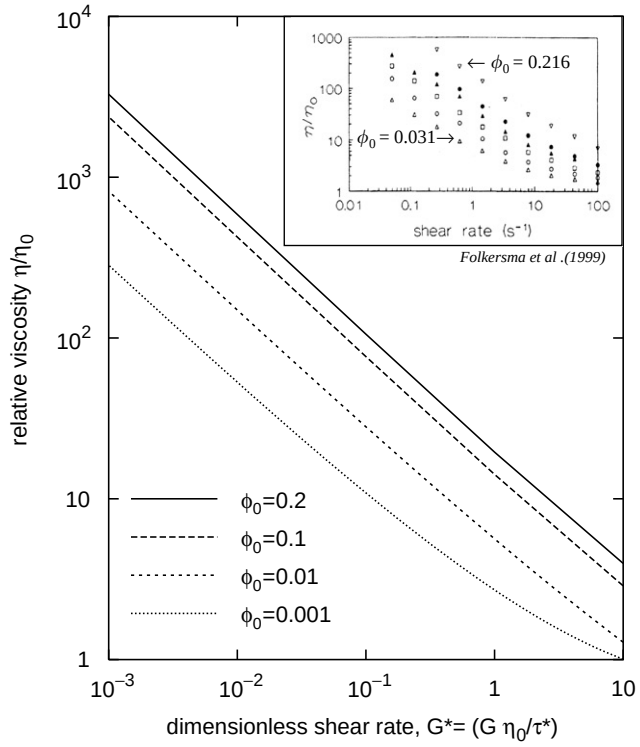

Fig. 6. Steady-state flow curves for various initial solids fractions or primary particle concentrations. Inset: experimental data adapted from Folkersma et al. (1999): flow curves for primary particle concentrations from $\phi_0 = 0.031$ ($\triangle$) to 0.216 (∇).

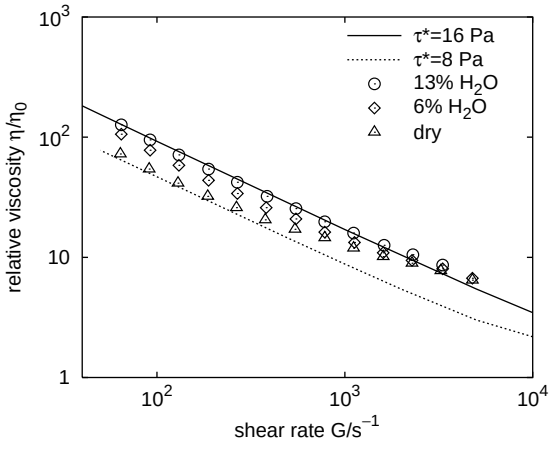

Fig. 7. Comparison between model predictions for the effect of varied particle interaction forces on flow curves (lines) and experimental results (dots) of Kurzbeck et al. (1996) of a pigment-wax suspension at 50°C at various moisture contents.

10%. A possible reason for this difference may be in the fragmentation kernel and that the coagulation kernel is derived for binary collisions without any influence of surrounding particles, which can lead to multiple collisions, enhancing coagulation and thus the viscosity.

Fig. 7 shows the effective suspension viscosity as a function of shear rate for τ^* equal to 8 Pa (dotted line) and 16 Pa (solid line) by the present model as well as the data

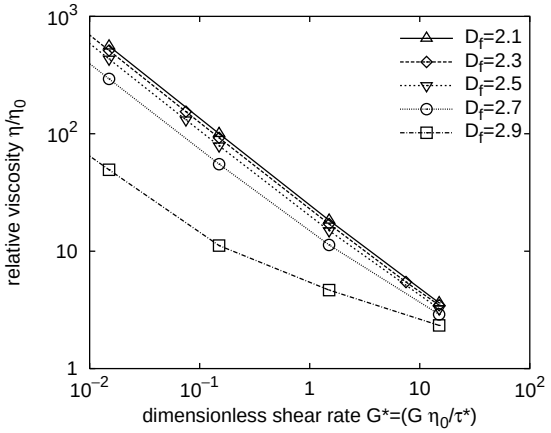

Fig. 8. Negligible influence of the fractal dimension in the typical range $D_f = 2.1$–2.7 on the flow curves for the system of Kurzbeck et al. (1996). Parameters: $\tau^* = 16$ Pa, otherwise as in Fig. 7.

of Kurzbeck et al. (1996) of a suspension of a hydrophobic molten wax at 50°C filled with a volume fraction ϕ_0=0.17 of chromium oxide pigment particles (d_p=5.1 μm) at different moisture content (points in Fig. 7). A variation of τ^* in the simulations leads to a parallel shift of the flow curves in the low shear rate range (Fig. 7), when the relative viscosity is plotted over the shear rate. The moisture enhances the aggregation of the particles. So increasing the moisture shifts the flow curves in the low shear rate range ($G < 300$ s^{-1}) parallel to higher viscosity. The τ^* is determined by matching the model predictions and experimental results. At higher shear rates, the experimentally measured effective viscosity decreases and approaches a value (at $G > 1000$ s^{-1}) above the viscosity of a completely deaggregated suspension. The highest applied shear stresses were apparently not sufficient to disintegrate the aggregates completely down to primary particles (Kurzbeck et al., 1996).

In the range of values that is typical for sheared suspensions ($D_f = 2.1$–2.7), the fractal dimension D_f has negligible influence on the slope of the flow curves of concentrated suspensions (Fig. 8). Only at fractal dimensions close to $D_f = 3$ the viscosity is reduced significantly. As $D_f \to 3$, the aggregates become more compact and immobilize less matrix liquid, and eventually none at all for $D_f = 3$. The insensitivity of the flow curves to the fractal dimension in the typical range for shear-induced aggregation (D_f = 2.1–2.7) indicates that the apparent viscosity is not significantly affected by the selection of D_f. Possible shear-induced restructuring, resulting in a compaction of aggregates and an increase of D_f over time, can be neglected for particles larger than 1 μm (Spicer et al., 1998; Selomulya, Bushell, Amal, & Waite, 2002).

Fig. 9 shows the effect of the fragmentation exponent q on the effective viscosity as a function of G^* for $q = 2$–6. The q changes the slope of the flow curve in contrast to the parallel shift of η_R by the previous parameters (ϕ_0, τ^* or D_f). This property of q facilitates the estimation from

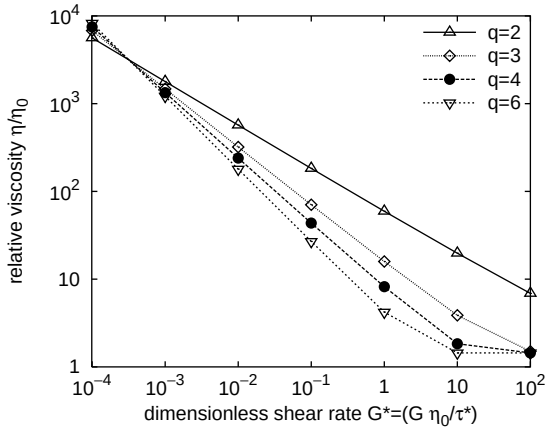

Fig. 9. Influence of the fragmentation exponent q on the slope of the simulated flow curves.

Table 2
Analysis of flow curves from literature

Author	Negative flow curve exponent	Calculated q
Experimental		
de Rooij et al. (1993): Fig. 3	0.64–0.84	2.8–6.4
Folkersma et al. (1999): Fig. 2	0.69–0.85	3.2–6.5
Kosmulski, Gustafsson, and Rosenholm (1999): Fig. 3	0.80	5.0
Kurzbeck et al. (1996): Fig. 6	0.71–0.79	3.4–4.7
Verduin, de Gans, and Dhont (1996): Table 1	0.43–0.77	1.75–4.3
Zaman et al. (1996): Fig. 1	0.55–0.84	2.2–6.4
Simulated		
Chen and Doi (1989): Fig. 14	0.56	2.3
Chen and Doi (1999): Fig. 11	0.67	3
Silbert, Melrose, and Ball (1997): Fig. 5	0.75	4
Silbert et al. (1999) (in text)	0.84	6.25

experimental data by regression of η at small G^*. There the flow curves can be approximated by the following power law correlation:

$$\eta_R \propto G^{(1-q)/q}. \tag{16}$$

Table 2 summarizes the analysis of flow curves in the literature. As the negative flow curve exponents scatter significantly (0.43–0.85), the extracted q also vary over some range ($q = 1.75$–6.5). Similar values (1.9–5.6) are reported by Serra and Casamitjana (1998) for dilute suspensions.

4. Summary and conclusions

A sectional population balance model for shear-induced coagulation fragmentation of concentrated suspensions is developed accounting for the immobilization of matrix liquid within the aggregates. This model describes the evolution of aggregate size distribution and the associated change of the suspension viscosity. The equilibrium aggregate size distributions are self-preserving with respect to the initial solids volume fraction and shear rate.

Flow curves of suspensions of polydisperse particles (up to 20% by solids volume) are calculated that are consistent with experimental data in the literature. The correlation between viscosity and shear rate can be described by a power law. Two material parameters are influencing significantly the predicted flow curves and need to be determined by comparison with experimental results: the fragmentation exponent q and the characteristic shear stress τ^*. The exponent q defines the sensitivity of the aggregates on the shear rate and is the only parameter with significant influence on the slope of the flow curves. The fractal dimension has little influence on the flow curves.

Notation

d	diameter (cm)
D_f	fractal dimension
G	shear rate (s^{-1})
k_b	dimension correction factor (1 cm^{-1} s^{-1})
N	aggregate number concentration (cm^{-3})
q	fragmentation exponent
S	fragmentation kernel (s^{-1})
t	time (s)
v	aggregate or particle volume (cm^3)
V	mass equivalent volume (of fully coalesced sphere) (cm^3)
x	number of primary particles per aggregate

Greek letters

β	collision kernel (cm^3 s^{-1})
Γ	fragment distribution function
η	dynamic viscosity (Pa s)
η_0	dynamic viscosity of matrix liquid (Pa s)
σ_g	geometric standard deviation of diameter (cm)
τ^*	characteristic shear stress (Pa)
ϕ	aggregate volume concentration

Superscripts and subscripts

c	collision
i, j	section number
m	maximum (concentration)
mm	mass mean
p	primary particle
R	relative
tot	total
0	initial, reference

Acknowledgements

This research was supported partially by the Deutsche Forschungsgemeinschaft (DFG, Grant No. Bu485/21-1) and the Swiss Commission for Technology and Innovation (KTI, TOP Nano21 Project No. 5773.2).

References

Barbé, J. C., Perez, M., & Papoular, M. (2000). Microstructure and viscosity of semi-solid mixtures. *Journal of Physics: Condensed Matter*, *12*(12), 2567–2577.

Blatz, P. J., & Tobolsky, A. V. (1945). Note on the kinetics of systems manifesting simultaneous polymerisation–depolymerisation phenomena. *Journal of Physical Chemistry*, *49*, 77–80.

Byrne, G. D. (1992). Pragmatic experiments with Krylov methods in the stiff ODE setting. In J. Cash & I. Gladwell (Eds.), *Computational ordinary differential equations* (pp. 323–356). Oxford: Oxford University Press.

Chen, D., & Doi, M. (1989). Simulation of aggregating colloids in shear flow. II. *Journal of Chemical Physics*, *91*(4), 2656–2663.

Chen, D., & Doi, M. (1999). Microstructure and viscosity of aggregating colloids under strong shearing force. *Journal of Colloid and Interface Science*, *212*(2), 286–292.

Coulaloglou, C. A., & Tavlarides, L. L. (1977). Description of interaction processes in agitated liquid–liquid dispersions. *Chemical Engineering Science*, *32*(11), 1289–1297.

Danov, K. D., Ivanov, I. B., Gurkov, T. D., & Borwankar, R. P. (1994). Kinetic-model for the simultaneous processes of flocculation and coalescence in emulsion systems. *Journal of Colloid and Interface Science*, *167*(1), 8–17.

de Rooij, R., Potanin, A. A., van den Ende, D., & Mellema, J. (1993). Steady shear viscosity of weakly aggregating polystyrene latex dispersions. *Journal of Chemical Physics*, *99*(11), 9213–9223.

de Rooij, R., Potanin, A. A., van den Ende, D., & Mellema, J. (1994). Transient shear viscosity of weakly aggregating polystyrene latex dispersions. *Journal of Chemical Physics*, *100*(7), 5353–5360.

Dickinson, E. (2000). Structure and rheology of simulated gels formed from aggregated colloidal particles. *Journal of Colloid and Interface Science*, *225*(1), 2–15.

Doi, M., & Chen, D. (1989). Simulation of aggregating colloids in shear flow. *Journal of Chemical Physics*, *90*(10), 5271–5279.

Flesch, R., Spicer, P. T., & Pratsinis, S. E. (1999). Laminar and turbulent shear-induced flocculation of fractal aggregates. *A.I.Ch.E. Journal*, *45*(5), 1114–1124.

Folkersma, R., van Diemen, A. J. G., Laven, J., van der Plas, G. A. J., & Stein, H. N. (1998). Visualization of the breakdown of dilute particle gels during steady-shear. *Rheologica Acta*, *37*, 549–555.

Folkersma, R., van Diemen, A. J. G., Laven, J., & Stein, H. N. (1999). Steady shear rheology of dilute polystyrene particle gels. *Rheologica Acta*, *38*, 257–267.

Graham, A. L., Steele, R. D., & Bird, R. B. (1984). Particle clusters in concentrated suspensions. 3. Prediction of suspension viscosity. *Industrial & Engineering Chemistry Fundamentals*, *23*(4), 420–425.

Gustafsson, J., Nordenswan, E., & Rosenholm, J. B. (2001). Shear-induced aggregation of anatase dispersions investigated by oscillation and low shear rate viscometry. *Journal of Colloid and Interface Science*, *242*(1), 82–89.

Happel, J., & Brenner, H. (1973). *Low Reynolds number hydrodynamics*. Leyden, Netherlands: Noordhoff.

Harris, S. J., & Maricq, M. M. (2002). The role of fragmentation in defining the signature size distribution of diesel soot. *Journal of Aerosol Science*, *33*(6), 935–942.

Higashitani, K., & Iimura, K. (1998). Two-dimensional simulation of the breakup process of aggregates in shear and elongational flows. *Journal of Colloid and Interface Science*, *204*, 320–327.

Hinds, W. C. (1999). *Aerosol Technology* (2nd ed.). New York: Wiley.

Horn, J. A., & Patterson, B. R. (1997). Thermally induced reversible coagulation in ceramic powder polymer liquid suspensions. *Journal of the American Ceramic Society*, *80*(7), 1789–1797.

Hounslow, M. J., Ryall, R. L., & Marshall, V. R. (1988). A discretized population balance for nucleation, growth, and aggregation. *A.I.Ch.E. Journal*, *34*(11), 1821–1832.

Ives, K. J. (1978). *The scientific basis of flocculation*. Alphen aan den Rijn, Netherlands: Sijthoff & Noordhoff.

Kim, S., & Karrila, S. J. (1991). *Microhydrodynamics*. London: Butterworth-Heinemann.

Kosmulski, M., Gustafsson, J., & Rosenholm, J. B. (1999). Correlation between the zeta potential and rheological properties of anatase dispersions. *Journal of Colloid and Interface Science*, *209*(1), 200–206.

Kramer, T. A., & Clark, M. M. (1999). Incorporation of aggregate breakup in the simulation of orthokinetic coagulation. *Journal of Colloid and Interface Science*, *216*(1), 116–126.

Kurzbeck, S., Kaschta, J., & Münstedt, H. (1996). Rheological behaviour of a filled wax system. *Rheologica Acta*, *35*, 446–457.

Lee, J.-D., So, J.-H., & Yang, S.-M. (1999). Rheological behavior and stability of concentrated silica suspensions. *Journal of Rheology*, *43*(5), 1117–1140.

Mandelbrot, B. B. (1983). *The fractal geometry of nature*. New York: Freeman.

Matsoukas, T., & Friedlander, S. K. (1991). Dynamics of aerosol agglomerate formation. *Journal of Colloid and Interface Science*, *146*(2), 495–506.

Netlib, (2001). *Netlib Repository at University of Tennessee and Oak Ridge National Laboratory*. URL: http://www.netlib.org/

Oles, V. (1992). Shear-induced aggregation and breakup of polystyrene latex particles. *Journal of Colloid and Interface Science*, *154*(2), 351–358.

Pandya, J. D., & Spielman, L. A. (1982). Floc breakage in agitated suspensions: Theory and data processing strategy. *Journal of Colloid and Interface Science*, *90*(2), 517–531.

Pandya, J. D., & Spielman, L. A. (1983). Floc breakage in agitated suspensions: Effect of agitation rate. *Chemical Engineering Science*, *38*(12), 1983–1992.

Quemada, D. (1977). Rheology of concentrated disperse systems. I. Minimum energy dissipation principle and viscosity–concentration relationship. *Rheologica Acta*, *16*(1), 82–94.

Quemada, D. (1998). Rheological modelling of complex fluids. I. The concept of effective volume fraction revisited. *European Physical Journal—Applied Physics*, *1*(1), 119–127.

Saffman, P., & Turner, J. (1956). On the collision of drops in turbulent clouds. *Journal of Fluid Mechanics*, *1*(1), 16–30.

Schmid-Schönbein, H., Gallasch, G., Gosen, J. V., Volger, E., & Klose, H. J. (1976). Redcell aggregation in blood flow. 2. Effect on apparent viscosity of blood. *Klinische Wochenschrift*, *54*(4), 159–167.

Selomulya, C., Bushell, G., Amal, R., & Waite, T. D. (2002). Aggregation mechanisms of latex of different particle sizes in a controlled shear environment. *Langmuir*, *18*, 1974–1984.

Serra, T., & Casamitjana, X. (1998). Effect of the shear and volume fraction on the aggregation and breakup of particles. *A.I.Ch.E. Journal*, *44*(8), 1724–1730.

Serra, T., Colomer, J., & Casamitjana, X. (1997). Aggregation and breakup of particles in a shear flow. *Journal of Colloid and Interface Science*, *187*, 466–473.

Silbert, L. E., Melrose, J. R., & Ball, R. C. (1997). Colloidal microdynamics: Pair-drag simulations of model-concentrated aggregated systems. *Physical Review E*, *56*(6), 7067–7077.

Silbert, L. E., Melrose, J. R., & Ball, R. C. (1999). The rheology and microstructure of concentrated, aggregated colloids. *Journal of Rheology*, *43*(3), 673–700.

Smoluchowski, M. von (1917). Versuch einer mathematischen Theorie der Koagulationskinetik kolloider Lösungen. *Zeitschrift für Physikalische Chemie*, *92*, 129–168.

Snabre, P., & Mills, P. (1996). I. Rheology of weakly flocculated suspensions of rigid particles. *Journal de Physique III*, *6*(12), 1811–1834.

Spicer, P. T., & Pratsinis, S. E. (1996a). Coagulation and fragmentation: Universal steady-state particle size distribution. *A.I.Ch.E. Journal*, *42*(6), 1612–1620.

Spicer, P. T., & Pratsinis, S. E. (1996b). Shear-induced flocculation: The evolution of floc structure and the shape of the size distribution at steady state. *Water Research*, *30*(5), 1049–1056.

Spicer, P. T., Pratsinis, S. E., Raper, J., Amal, R., Bushell, G., & Meesters, G. (1998). Effect of shear schedule on particle size, density, and structure during flocculation in stirred tanks. *Powder Technology*, *97*, 26–34.

Spicer, P. T., Pratsinis, S. E., Trennepohl, M. E., & Meesters, G. H. M. (1996). Coagulation and fragmentation: The variation of shear rate and the time lag for attainment of steady state. *Industrial & Engineering Chemistry Research*, *35*(9), 3074–3080.

Tang, S., Ma, Y., & Shiu, C. (2001). Modelling the mechanical strength of fractal aggregates. *Colloids and Surfaces A*, *180*(1–2), 7–16.

Tsutsumi, A., Yoshida, K., Yui, M., Kanamori, S., & Shibata, K. (1994). Shear viscosity behavior of flocculated suspensions. *Powder Technology*, *78*(2), 165–172.

van de Ven, T. G. M. (1989). *Colloidal hydrodynamics*. London: Academic Press.

Vanni, M., & Baldi, G. (2002). Coagulation efficiency of colloidal particles in shear flow. *Advances in Colloid and Interface Science*, *97*(1–3), 151–177.

Varadan, P., & Solomon, M. J. (2001). Shear-induced microstructural evolution of a thermoreversible colloidal gel. *Langmuir*, *17*(10), 2918–2929.

Veerapaneni, S., & Wiesner, M. R. (1996). Hydrodynamics of fractal aggregates with radially varying permeability. *Journal of Colloid and Interface Science*, *177*, 45–57.

Vemury, S., & Pratsinis, S. E. (1995). Self-preserving size distributions of agglomerates. *Journal of Aerosol Science*, *26*(4), 175–185.

Verduin, H., de Gans, B. J., & Dhont, J. K. G. (1996). Shear induced structural changes in a gel-forming suspension studied by light scattering and rheology. *Langmuir*, *12*(12), 2947–2955.

Weipert, D., Tscheuschner, H. D., & Windhab, E. (1993). *Rheologie der Lebensmittel*. Hamburg, Germany: Behr's.

Wolthers, W., van den Ende, D., Duits, M. H. G., & Mellema, J. (1996). The viscosity and sedimentation of aggregating colloidal dispersions in a Couette flow. *Journal of Rheology*, *40*(1), 55–67.

Zaman, A. A., Moudgil, B. M., Fricke, A. L., & El-Shall, H. (1996). Rheological behavior of highly concentrated aqueous silica suspensions in the presence of sodium nitrate and polyethylene oxide. *Journal of Rheology*, *40*(6), 1191–1210.